2014-08

A new tetracyclic lactam building block for thick, broad-bandgap photovoltaics

Journal of the American Chemical Society,Washington, DC: American Chemical Society - ACS,v. 136, n. 33, p. 11578-11581, Aug. 2014

http://www.producao.usp.br/handle/BDPI/50204

JACS
JOURNAL OF THE AMERICAN CHEMICAL SOCIETY
Communication
pubs.acs.org/JACS

A New Tetracyclic Lactam Building Block for Thick, Broad-Bandgap Photovoltaics

Renee Kroon,*[,†,‡] Amaia Diaz de Zerio Mendaza,[‡] Scott Himmelberger,[§] Jonas Bergqvist,[∥] Olof Bäcke,[⊥] Gregório Couto Faria,[§,#] Feng Gao,[∥] Abdulmalik Obaid,[▽] Wenliu Zhuang,[‡] Desta Gedefaw,[‡] Eva Olsson,[⊥] Olle Inganäs,[∥] Alberto Salleo,[§] Christian Müller,*[,‡] and Mats R. Andersson[†,‡]

[†]Ian Wark Research Institute, University of South Australia, Adelaide, SA 5095, Australia

[‡]Department of Chemical and Biological Engineering and [⊥]Department of Applied Physics, Chalmers University of Technology, 41296 Göteborg, Sweden

[§]Department of Materials Science and Engineering, Stanford University, Stanford, California 94305, United States

[∥]Department of Physics, Chemistry and Biology, Linköping University, 58183 Linköping, Sweden

[#]Instituto de Física de São Carlos, Universidade de São Paulo, São Carlos, SP 13560-970, Brazil

[▽]Department of Physics, Wake Forest University, Winston-Salem, North Carolina 27106, United States

Supporting Information

ABSTRACT: A new tetracyclic lactam building block for polymer semiconductors is reported that was designed to combine the many favorable properties that larger fused and/or amide-containing building blocks can induce, including improved solid-state packing, high charge carrier mobility, and improved charge separation. Copolymerization with thiophene resulted in a semicrystalline conjugated polymer, PTNT, with a broad bandgap of 2.2 eV. Grazing incidence wide-angle X-ray scattering of PTNT thin films revealed a strong tendency for face-on π-stacking of the polymer backbone, which was retained in PTNT:fullerene blends. Corresponding solar cells featured a high open-circuit voltage of 0.9 V, a fill factor around 0.6, and a power conversion efficiency as high as 5% for >200 nm thick active layers, regardless of variations in blend stoichiometry and nanostructure. Moreover, efficiencies of >4% could be retained when thick active layers of ∼400 nm were employed. Overall, these values are the highest reported for a conjugated polymer with such a broad bandgap and are unprecedented in materials for tandem and particularly ternary blend photovoltaics. Hence, the newly developed tetracyclic lactam unit has significant potential as a conjugated building block in future organic electronic materials.

Organic solar cells (OSCs) continue to attract scientific interest because they offer the prospect of an economically feasible high-throughput production process.[1] Extensive research efforts using laboratory-scale devices—primarily incorporating photoactive layers based on polymer:fullerene blends—have already led to benchmark efficiencies of 9−10%.[2] Meanwhile, important advances have been made with regard to tuning high-throughput techniques such as roll-to-roll processing, inkjet-printing, or spray-coating for large-scale production of OSCs.[3]

Employing thick active layers in OSCs is of outmost importance, as it would solve a number of issues in photovoltaic devices. For instance, to ensure reproducibility in large-area OSC production, deposition of a thick active layer (>200 nm) is preferred because it allows for the formation of more-uniform films with a lower defect density (pinholes).[4] Additionally, increasing the active layer thickness enhances the number of absorbed photons and thus, potentially, the extracted photocurrent. For very thick active layers (>400 nm), the optical absorption becomes nearly impervious to destructive interference, which further enhances the reproducibility of OSCs.[5] Aside from offering a high open-circuit voltage (V_{oc}), broad bandgap materials for tandem cells ideally enable the deposition of thick active layers, as a high but invariant short-circuit current density (J_{sc}) for one cell would allow for easier optimization of the second subcell's current density at the maximum power point (MPP).[6] Furthermore, materials that enable thick photoactive layers are usually characterized by high charge carrier mobilities, which would benefit charge transport (CT) and optical density in OSCs incorporating sensitizer-based ternary blends.[7]

Unfortunately, most OSCs incorporate materials that offer optimized power conversion efficiencies (PCEs) when ∼100 nm thick active layers are employed. Increasing the active layer thickness usually causes increased internal resistance and space charge limited currents, aggravating bimolecular recombination. This is expressed in a reduced fill factor (FF) that is consequently detrimental to the photovoltaic performance.[8]

So far, only a limited number of donor polymers have been reported that can be used in OSCs with thick polymer:fullerene active layers but high FFs and PCEs. The most widely studied are regioregular poly(3-hexylthiophene) (P3HT) and phenyl-C_{61}-butyric acid methyl ester (PCBM), which continue to perform well with an active layer >200 nm.[5,9] Recently, other, more exotic polymer structures have been reported that also enable thick polymer:fullerene active layers in OSCs. For instance, high-performance diketopyrrolopyrrole copolymer:fullerene-based OSCs with a thickness up to 400 nm were reported by Li et

Received: May 23, 2014
Published: July 24, 2014

   dx.doi.org/10.1021/ja5051692 | J. Am. Chem. Soc. 2014, 136, 11578−11581

Scheme 1. Synthetic Route toward NT and PTNT[a]

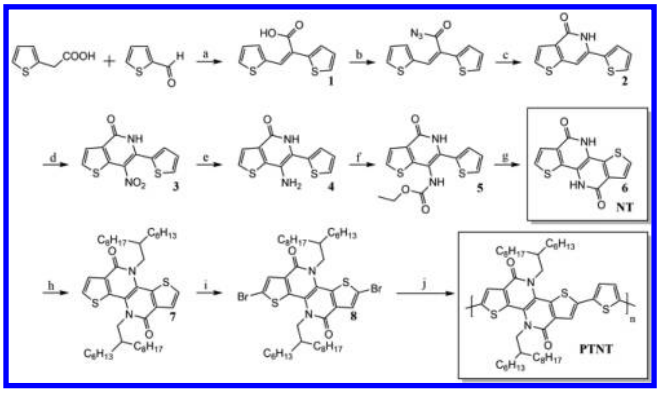

[a]Reagents and conditions: (a) Ac_2O, triethylamine, 150 °C; (b) step 1, oxalyl chloride, acetone, 0 °C; step 2, NaN_3(aq), 0 °C; (c) Bu_3N, diphenyl ether, 250 °C; (d) HNO_3, AcOH, EtAc; (e) Pd/C, H_2, THF, 30 °C; (f) ethyl chloroformate, Et_3N, THF, 0 °C; (g) Bu_3N, diphenyl ether, 250 °C; (i) K_2CO_3, 2-HDBr, KI, DMF, 90 °C; (j) NBS, AcOH, $CHCl_3$, 50 °C; (h) 2,5-bis(trimethylstannyl)thiophene, $Pd_2(dba)_3$, P(*o*-Tol)$_3$, toluene, 90 °C.

al.[10] However, the best donor polymers reported to date are based on benzotriazole, thiazolothiazole, or naphtha-bisbenzothiadiazole units, which not only sustain a maximum PCE ≈ 6−9% for 200−280 nm layers but also can give 1 μm thick active layers with PCE ≈ 6−8%.[11]

Here we describe the synthesis and characterization of a new polymer, poly(2,5-thiophene-*alt*-4,9-bis(2-hexyldecyl)-4,9-dihydrodithieno[3,2-*c*:3′,2′-*h*][1,5]naphthyridine-5,10-dione) (PTNT), which yields high OSC efficiencies in devices with thick active layers. PTNT is a broad bandgap polymer that incorporates the novel unit 4,9-bis(2-hexyldecyl)-4,9-dihydrodithieno[3,2-*c*:3′,2′-*h*][1,5]naphthyridine-5,10-dione (NT), a tetracyclic fused lactam ring that was designed to combine the many favorable properties that larger fused and/or amide-containing building blocks can induce, such as improved solid-state packing, high charge carrier mobility, and improved charge separation.[12] Poduval et al. and Cao et al. recently adopted the same strategy;[13] particularly the work of Cao et al. shows the feasibility of this strategy, reporting OSCs with 8% PCE. PTNT enables the fabrication of OSCs with PCEs as high as 5% and thus represents a valuable addition to the growing library of polymer semiconductors.

A synthetic route previously reported by Bisagni et al.[14] was modified for the synthesis of NT and PTNT (Scheme 1; see SI for synthetic details). First, 2-thiopheneacetic acid and 2-thiophene carboxaldehyde were reacted via Perkin condensation to yield **1**.[15] We found that a second crop of the *E*-isomer could be obtained by heating the *Z*-isomer for 4 days under the same reaction conditions.[16] In this way, a batch process for the *E*-isomer can be created which mitigates the low yield of this reaction. After formation of the acyl azide, conversion via Curtius rearrangement at high temperatures gave the intermediate isocyanate, which, under these conditions, immediately converted to **2**. Nitration of **2** at low temperature seemed to be selective for the proton on the 7-position and offered **3**. Reduction with hydrogen + Pd/C then resulted in **4**. Subsequent reaction with ethyl chloroformate offered the pending carbamate group (**5**). Subjecting **5** to high temperatures caused nucleophilic attack of the thiophene to the carbonyl, after which the NT unit **6** was obtained. We note that, up to this point, no extensive purification was necessary, which makes NT suitable for up-scaling. **6** can then be *N*-alkylated with an alkyl bromide, in this work 2-hexyldecyl bromide, to ensure solubility (**7**). To brominate the alkylated monomer, we found that slightly elevated temperatures and a catalytic amount of acetic acid were necessary to drive the reaction and form **8**. After purification, **8** was polymerized with 2,5-bis(trimethylstannyl)-thiophene to yield PTNT.

PTNT is soluble in solvents such as toluene, chloroform, chlorobenzene, and in particular *ortho*-dichlorobenzene (*o*-DCB), which permits the dissolution of higher concentrations of 10−20 g/L. The molecular weight was determined via size exclusion chromatography in 1,2,4-trichlorobenzene (1,2,4-TCB) at 150 °C. For both a relative calibration against polystyrene and universal calibration, high number-average molecular weights were found, $M_n \approx 45$ kg/mol (PDI = 3.5) and $M_n \approx 38$ kg/mol (PDI = 2.9), respectively. Moreover, linearization of the Mark−Houwink−Sakurada equation $[\eta] = KM^{\alpha}$, where $[\eta]$ is the intrinsic viscosity and K and α are parameters, yielded $K = 122 \times 10^{-5}$ dL/g and $\alpha = 0.5$ (SI), indicating theta solvent conditions for PTNT in 1,2,4-TCB at 150 °C.

The oxidation and reduction potentials of PTNT, $V_{ox}^{onset} = 0.81$ V and $V_{red}^{onset} = -1.56$ V (SI) vs Fc/Fc^+, were measured by square-wave voltammetry, yielding an electrochemical bandgap $E_g^{ec} = 2.37$ eV. From these values the HOMO and LUMO were estimated to be −5.94 and −3.57 eV, respectively. UV/vis absorption spectra of *o*-DCB solutions as well as thin solid films reveal an absorption onset of only 560 nm (Figure 1a), which corresponds to a broad solid-state optical bandgap of 2.2 eV. When PTNT is blended with PCBM, the broad bandgap and deep HOMO can be expected to result in a high photovoltage, which would make PTNT a suitable material for tandem solar cells. Additionally, the broad bandgap of PTNT results in solid-state emission in the visible range of the spectrum.

Initially, we probed the ability of PTNT to order by melting 1,3,5-trichlorobenzene (1,3,5-TCB) crystals on a thick PTNT film, which dissolves the polymer. During cooling of the liquid 1,3,5-TCB, this typically results in partial alignment of semicrystalline conjugated polymers by directional epitaxial

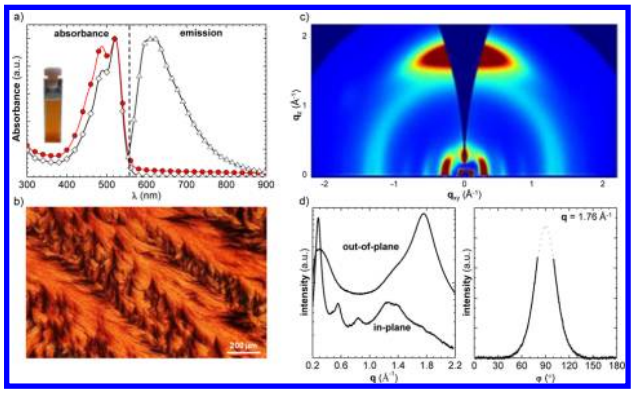

Figure 1. Physicochemical properties of PTNT. (a) Optical absorption of PTNT in *o*-DCB solution (red circles) + neat films (open diamonds) and solid-state photoluminescence. (b) Polarized optical microscopy images of 1,3,5-TCB nucleated PTNT samples on a glass substrate (5× magnification). (c) 2D-GIWAXS pattern of neat PTNT. (d) In-plane and out-of-plane GIWAXS scans (left) and pole figures (right) of the polymer π-stacking peak at $q = 1.76$ Å^{-1} with Gaussian fit curve (gray dotted line).

dx.doi.org/10.1021/ja5051692 | J. Am. Chem. Soc. 2014, 136, 11578−11581

crystallization on solidified 1,3,5-TCB crystallites, followed by removal of 1,3,5-TCB through sublimation.[17] Indeed, polarized optical microscopy revealed distinct birefringent structures (Figure 1b), confirming the presence of ordered polymer domains that persisted at temperatures as high as 300 °C (SI).

To characterize the solid-state order of PTNT in detail, we carried out grazing incidence wide-angle X-ray scattering (GIWAXS) on neat polymer films that were spin-coated from *o*-DCB (Figure 1c and SI). A distinct signal at $q_{010} \approx 1.76$ Å^{-1} in the out-of-plane direction is assigned to π-stacking, which corresponds to a short π-stacking distance, $d_{010} = 2\pi/q_{010} \approx 3.57$ Å, assuming that PTNT crystallizes with an orthorhombic unit cell. The out-of-plane orientation of q_{010} indicates a predominantly face-on orientation of PTNT with respect to the silicon substrate. Pole figures of the π-stacking peak (Figure 1d) were used to extract a Herman's orientation factor with a high value of $S_{010} \approx 0.89$, where $S_{010} = 1$ corresponds to perfect out-of-plane alignment and $S_{010} = 0$ to an isotropic distribution of crystallites, indicating a strong tendency of PTNT crystals to order face-on with respect to the silicon substrate. Moreover, three orders of the lamellar diffraction peak at $q_{100} \approx 0.28$ Å^{-1}, $q_{200} \approx 0.55$ Å^{-1}, and $q_{300} \approx 0.85$ Å^{-1} are apparent in the in-plane direction, which correspond to an interchain spacing of 22.1 Å. Coherence lengths of $D_{010} \approx 2.4$ nm and $D_{100} \approx 12.6$ nm were calculated via the Scherrer equation, corresponding to ordering of 5−6 and 6−7 PTNT segments in the π-stacking and lamellar-stacking direction, respectively. Pure PTNT was used in field-effect transistors (FETs), which showed hole-only transport with moderate values of $(2-3) \times 10^{-3}$ cm^2/(V·s) (SI), likely due to the perpendicular stacking of PTNT with respect to the lateral CT in FETs.

A conventional solar cell device architecture comprising ITO/PEDOT:PSS/active layer/LiF/Al was employed to evaluate the photovoltaic performance of 1:1, 2:3, and 1:2 PTNT:$PC_{71}BM$ blends. Active layers were spin-coated from *o*-DCB due to the superior solubility of PTNT in this solvent.

To investigate the influence of blend nanostructure on the photovoltaic performance, we compared a set of neat blends, spin-coated from *o*-DCB, and blends processed from *o*-DCB with addition of 3% of the "processing additive" diiodooctane (DIO). Spin-coating of PTNT:$PC_{71}BM$ photovoltaic active layer blends from *o*-DCB readily resulted in the formation of smooth thin films, as evidenced by a low root-mean-square roughness of 1.6 ± 0.2 nm, obtained by atomic force microscopy (AFM) for 2:3 PTNT:$PC_{71}BM$ films. AFM and transmission electron microscopy (TEM) revealed the existence of 50−100 nm small domains in neat blend films (Figure 2a,c), in contrast to significantly more fine-grained DIO-processed active layers (Figure 2b,d). GIWAXS of a 2:3 PTNT:$PC_{71}BM$ film revealed that the tendency of PTNT to order persists upon blending with $PC_{71}BM$

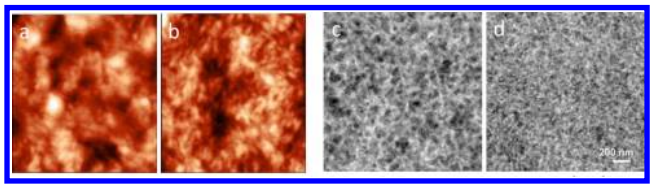

Figure 2. Morphology of PTNT:$PC_{71}BM$ blends. AFM height images (left) and TEM bright-field micrographs (right) of the active layer in photovoltaic devices of (a,c) 2:3 PTNT:$PC_{71}BM$ and (b,d) 2:3 PTNT:$PC_{71}BM$ processed with 3% DIO. Root-mean-square values of 1.6 ± 0.2 nm. The scale bar is representative for all images.

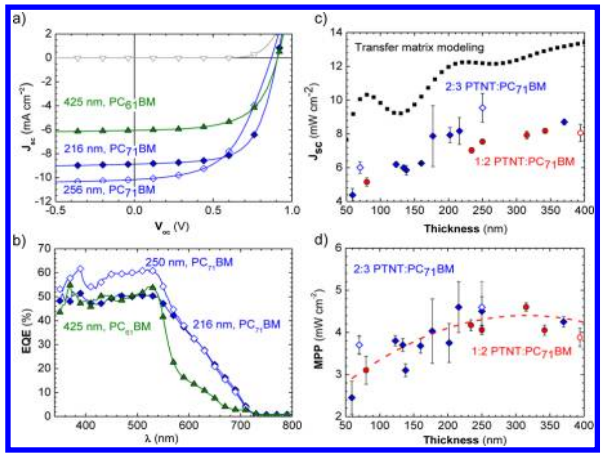

Figure 3. PTNT:fullerene photovoltaic characteristics: (a) *J*−*V* and (b) EQE of 2:3 PTNT:$PC_{71}BM$-based (blue diamonds) and 1:2 PTNT:$PC_{61}BM$-based (green triangles) OSCs; (c) J_{sc}, including values from transfer matrix modeling (black squares); and (d) MPP as a function of active layer thickness for 1:2 (red circles) and 2:3 PTNT:$PC_{71}BM$-based devices. Red line functions as guide to the eye. Open/closed symbols correspond to devices with/without DIO.

(SI). Similar to neat PTNT, blend films are characterized by lamellar- and π-stacking signals at 0.28 and 1.76 Å^{-1}, respectively. Moreover, we observe a high Herman's orientation factor $S \approx 0.82$, indicating a strong preference for face-on stacking of the polymer backbone with respect to the substrate, which according to literature benefits vertical CT across the active layer.[11b,18] To obtain a measure for the majority charge-carrier mobility of the blend, devices were probed with photo-charge extraction by linearly increasing voltage, which yielded values of $(1-2) \times 10^{-4}$ cm^2/(V·s) (SI). Despite the strong effect of DIO on the blend nanostructure, for 2:3 PTNT:$PC_{71}BM$ layers with similar thickness, the external quantum efficiency (EQE) increased from only ∼50% to ∼60% in the 350−550 nm absorption region and resulted in a small increase in J_{sc} by ∼1.5 mA cm^{-2}. This improvement was accompanied by a slight drop in V_{oc} by 0.04 V and a substantial decrease in FF (Figure 3a,b). The slight drop in V_{oc} can be explained by an enhanced solid-state order of the polymer that such processing agents can induce, which then would lower the CT energy and slightly reduce the V_{oc}.[19] Overall, the MPP remained virtually unchanged (SI); we therefore conclude that the PCE of PTNT:$PC_{71}BM$ is relatively robust with regard to changes in nanostructure.

To investigate the influence of film thickness, in a further set of experiments we prepared active layers ranging from 60 to 395 nm thick by adjusting the blend solution concentration and spin-coating speed (Figure 3c,d). Independent of the active layer thickness, the devices were characterized by an invariant $V_{oc} \approx 0.9$ V. The FF decreased only slightly with increasing film thickness: thinner active layers (60−200 nm) had FF ≈ 0.68−0.60, whereas thicker films (200−400 nm) had FF ≈ 0.60−0.54. J_{sc} was more strongly affected by changes in active layer thickness. For both 1:2 and 2:3 PTNT:$PC_{71}BM$ we note two regimes, one at 60−170 nm with a low $J_{sc} \approx 5-6$ mA/cm^2 and a second one at 180−400 nm with an improved $J_{sc} \approx 7-10$ mA/cm^2. Transfer matrix modeling on a 1:2 PTNT:$PC_{71}BM$ film revealed that these two regimes coincide with the first and second interference minima at thicknesses of 80 and 220 nm, respectively. Thus, the typical internal quantum efficiency is between 60 and 70%. Overall, MPP = 4−5 mW/cm^2 is retained for a broad range of thicknesses (200−400 nm).

dx.doi.org/10.1021/ja5051692 | *J. Am. Chem. Soc.* 2014, 136, 11578−11581

The EQE spectra of PTNT:$PC_{71}BM$ devices feature a strong signal between 560 and 700 nm due to the good absorption of $PC_{71}BM$ in this region (Figure 3b). For parallel-connected tandem solar cells, transparency in this region is required, which can be readily achieved by instead using $PC_{61}BM$ as the acceptor material. Indeed, EQE spectra of PTNT:$PC_{61}BM$ devices offer improved transparency above the bandgap of PTNT. Nevertheless, a promising MPP > 3 mW/cm^2 could be maintained for active layers as thick as 425 nm (SI).

We have reported the synthesis of a new tetracyclic lactam acceptor unit, NT, for conjugated polymers, which is characterized by a high degree of planarity. Copolymerization with thiophene resulted in the donor polymer PTNT, which has a broad bandgap of only 2.2 eV. Optical microscopy and GIWAXS revealed that PTNT is semicrystalline and predominantly orders face-on in thin films, which persists upon blending with fullerenes. As a result, OSCs based on PTNT:fullerene blends offer a good photovoltaic performance, with $V_{oc} \approx 0.9$ V and a PCE up to 5% that is relatively robust with regard to variations in active layer thickness up to 400 nm as well as blend stoichiometry and nanostructure. Varying processing parameters, such as thermal or vapor annealing as well as energy level engineering, are likely to result in further gains in photovoltaic performance of PTNT-based OSCs. Furthermore, active layers up to 425 nm thick still resulted in PCE ≈ 3% for PTNT:$PC_{61}BM$-based devices. We attribute these favorable physicochemical and optoelectronic properties of PTNT to the incorporation of the NT unit; thus, we conclude that the novel NT unit is a promising building block for donor polymers. The combined properties of PTNT are unprecedented, which makes PTNT an outstanding material for use in tandem solar cells and, in particular, ternary blend photovoltaics.

■ ASSOCIATED CONTENT

Supporting Information

Experimental details and characterization data and images. This material is available free of charge via the Internet at http://pubs.acs.org.

■ AUTHOR INFORMATION

Corresponding Authors

renee.kroon@unisa.edu.au
christian.muller@chalmers.se

Notes

The authors declare no competing financial interest.

■ ACKNOWLEDGMENTS

We thank the Chalmers Areas of Advance Materials Science, Energy and Nanoscience and Nanotechnology as well as the Swedish Research Council and Formas for funding. R.K. acknowledges the Swedish Energy Agency for financial support. A.D. was supported by the Linnaeus Centre for Bioinspired Supramolecular Function and Design. S.H. thanks the National Science Foundation for assistance in the form of a Graduate Research Fellowship. Use of the Stanford Synchrotron Radiation Lightsource, SLAC National Accelerator Laboratory, is supported by the U.S. Department of Energy, Office of Science, Office of Basic Energy Sciences under Contract No. DE-AC02-76SF00515.

■ REFERENCES

(1) Espinosa, N.; Hosel, M.; Angmo, D.; Krebs, F. C. *Energy Environ. Sci.* **2012**, *5*, 5117.

(2) (a) He, Z.; Zhong, C.; Su, S.; Xu, M.; Wu, H.; Cao, Y. *Nat. Photonics* **2012**, *6*, 591. (b) You, J.; Dou, L.; Yoshimura, K.; Kato, T.; Ohya, K.; Moriarty, T.; Emery, K.; Chen, C.; Gao, J.; Li, G.; Yang, Y. *Nat. Commun.* **2013**, *4*, 1446.

(3) Søndergaard, R. R.; Hösel, M.; Krebs, F. C. *J. Polym. Sci., Part B: Polym. Phys.* **2013**, *51*, 16.

(4) (a) Lee, J.-H.; Sagawa, T.; Yoshikawa, S. *Thin Solid Films* **2013**, *529*, 464. (b) Li, G.; Shrotriya, V.; Huang, J.; You, Y.; Moriarty, T.; Emery, K.; Yang, Y. *Nat. Mater.* **2005**, *4*, 864.

(5) Dennler, G.; Scharber, M. C.; Brabec, C. J. *Adv. Mater.* **2009**, *21*, 1323.

(6) Ameri, T.; Li, N.; Brabec, C. J. *Energy Environ. Sci.* **2013**, *6*, 2390.

(7) Ameri, T.; Khoram, P.; Min, J.; Brabec, C. J. *Adv. Mater.* **2013**, *25*, 4245.

(8) (a) Moulé, A. J.; Bonekamp, J. B.; Meerholz, K. *J. Appl. Phys.* **2006**, *100*, 094503. (b) Lenes, M.; Koster, L. J. A.; Mihailetchi, V. D.; Blom, P. W. M. *Appl. Phys. Lett.* **2006**, *88*, 243502.

(9) Lee, S.; Nam, S.; Kim, H.; Kim, Y. *Appl. Phys. Lett.* **2010**, *97*, 103503.

(10) Li, W.; Hendriks, K. H.; Roelofs, W. S. C.; Kim, Y.; Wienk, M. M.; Janssen, R. A. J. *Adv. Mater.* **2013**, *25*, 3182.

(11) (a) Price, S. C.; Stuart, A. C.; Yang, L.; Zhou, H.; You, W. *J. Am. Chem. Soc.* **2011**, *133*, 4625. (b) Osaka, I.; Saito, M.; Koganezawa, T.; Takimiya, K. *Adv. Mater.* **2014**, *26*, 331. (c) Hu, X.; Yi, C.; Wang, M.; Hsu, C.; Liu, S.; Zhang, K.; Zhong, C.; Huang, F.; Gong, X.; Cao, Y. *Adv. Energy Mater.* **2014**, 201400378.

(12) (a) Zhang, X.; Richter, L. J.; DeLongchamp, D. M.; Kline, R. J.; Hammond, M. R.; McCulloch, I.; Heeney, M.; Ashraf, R. S.; Smith, J. N.; Anthopoulos, T. D.; Schroeder, B.; Geerts, Y. H.; Fischer, D. A.; Toney, M. F. *J. Am. Chem. Soc.* **2011**, *133*, 15073. (b) Bronstein, H.; Chen, Z.; Ashraf, R. S.; Zhang, W.; Du, J.; Durrant, J. R.; Shakya Tuladhar, P.; Song, K.; Watkins, S. E.; Geerts, Y.; Wienk, M. M.; Janssen, R. A. J.; Anthopoulos, T. D.; Sirringhaus, H.; Heeney, M.; McCulloch, I. *J. Am. Chem. Soc.* **2011**, *133*, 3272. (c) Chen, Z.; Zheng, Y.; Yan, H.; Facchetti, A. *J. Am. Chem. Soc.* **2008**, *131*, 8. (d) Zheng, Q.; Jung, B. J.; Sun, J.; Katz, H. E. *J. Am. Chem. Soc.* **2010**, *132*, 5394. (e) Biniek, L.; Schroeder, B. C.; Donaghey, J. E.; Yaacobi-Gross, N.; Ashraf, R. S.; Soon, Y. W.; Nielsen, C. B.; Durrant, J. R.; Anthopoulos, T. D.; McCulloch, I. *Macromolecules* **2013**, *46*, 727. (f) Xu, Y.-X.; Chueh, C.-C.; Yip, H.-L.; Ding, F.-Z.; Li, Y.-X.; Li, C.-Z.; Li, X.; Chen, W.-C.; Jen, A. K. Y. *Adv. Mater.* **2012**, *24*, 6356. (g) Chang, C.-Y.; Cheng, Y.-J.; Hung, S.-H.; Wu, J.-S.; Kao, W.-S.; Lee, C.-H.; Hsu, C.-S. *Adv. Mater.* **2012**, *24*, 549. (h) Schwarz, C.; Bässler, H.; Bauer, I.; Koenen, J.-M.; Preis, E.; Scherf, U.; Köhler, A. *Adv. Mater.* **2010**, *24*, 922.

(13) (a) Poduval, M. K.; Burrezo, P. M.; Casado, J.; López Navarrete, J. T.; Ortiz, R. P.; Kim, T. *Macromolecules* **2013**, *46*, 9220. (b) Cao, J.; Liao, Q.; Du, X.; Chen, J.; Xiao, Z.; Zuo, Q.; Ding, L. *Energy Environ. Sci.* **2013**, *6*, 3224.

(14) Bisagni, E.; Landras, C.; Thirot, S.; Huel, C. *Tetrahedron* **1996**, *52*, 10427.

(15) Pavlicic, D.; Koružnjak, J.; Banic-Tomišic, Z.; Karminski-Zamola, G. *Molecules* **2002**, *7*, 871.

(16) Pálinkó, I.; Török, B.; Tasi, G.; Körtvélyesi, T. In *Electronic Conferences on Trends in Organic Chemistry (ECTOC-1)*; Rzepa, H. S., Goodman, J. M., Leach, C., Eds.; Royal Society of Chemistry: London, 1995; http://www.ch.ic.ac.uk/ectoc/ectoc-1.html.

(17) Müller, C.; Aghamohammadi, M.; Himmelberger, S.; Sonar, P.; Garriga, M.; Salleo, A.; Campoy-Quiles, M. *Adv. Funct. Mater.* **2013**, *23*, 2368.

(18) Gomez, E. D.; Barteau, K. P.; Wang, H.; Toney, M. F.; Loo, Y.-L. *Chem. Commun.* **2011**, *47*, 436.

(19) Vandewal, K.; Gadisa, A.; Oosterbaan, W. D.; Bertho, S.; Banishoeib, F.; van Severen, I.; Lutsen, L.; Cleij, T. J.; Vanderzande, D.; Manca, J. V. *Adv. Funct. Mater.* **2008**, *18*, 2064.